

Channel Estimation in MIMO Systems Aided by Microwave Linear Analog Computers (MiLACs)

Qiaosen Zhang, Matteo Nerini, *Member, IEEE*, Bruno Clerckx, *Fellow, IEEE*

Abstract—Microwave linear analog computers (MiLACs) have recently emerged as a promising solution for future gigantic multiple-input multiple-output (MIMO) systems, enabling beamforming with greatly reduced hardware and computational cost. However, channel estimation for MiLAC-aided systems remains an open problem. Conventional least squares (LS) and minimum mean square error (MMSE) estimation rely on intensive digital computation, which undermines the benefits offered by MiLACs. In this letter, we propose efficient LS and MMSE channel estimation schemes for MiLAC-aided MIMO systems. By designing training precoders and combiners implemented by MiLACs, both LS and MMSE estimation are performed fully in the analog domain, achieving identical performance to their digital counterparts while significantly reducing computational complexity, transmit RF chains, analog-to-digital/digital-to-analog converters (ADCs/DACs) resolution requirements, and peak-to-average power ratio (PAPR). Numerical results verify the effectiveness and advantages of the proposed schemes.

Index Terms—Channel estimation, microwave linear analog computer (MiLAC), multiple-input multiple-output (MIMO).

I. INTRODUCTION

FROM second-generation (2G) to fifth-generation (5G), wireless networks have witnessed a steady evolution towards large-scale multiple-input multiple-output (MIMO) architectures, progressing from a few antennas to tens or even hundreds. This evolution enables substantial throughput gains via enhanced beamforming and spatial multiplexing, which are expected to be further strengthened in sixth-generation (6G) networks with the emergence of gigantic MIMO employing thousands of antennas [1], [2].

Scaling up antenna numbers makes conventional digital beamforming increasingly impractical, as it requires a dedicated radio-frequency (RF) chain per antenna, resulting in prohibitive hardware cost, computational complexity, and power consumption. To tackle these challenges, recent research has focused on alternative beamforming strategies that shift computation from the conventional digital domain to the more efficient analog domain. Among these strategies, microwave linear analog computer (MiLAC)-aided beamforming has recently emerged as a compelling candidate [3], [4]. A MiLAC is a multiport microwave network composed of tunable admittance components capable of processing microwave signals entirely in the analog domain, hence realizing arbitrary beamforming.

Qiaosen Zhang, Matteo Nerini, and Bruno Clerckx are with the Department of Electrical and Electronic Engineering, Imperial College London, SW7 2AZ London, U.K (e-mail: qiaosen.zhang23@imperial.ac.uk; m.nerini20@imperial.ac.uk; b.clerckx@imperial.ac.uk).

This approach offers maximum flexibility comparable to digital beamforming while substantially reducing computational complexity, requiring only a minimal number of RF chains and low-resolution analog-to-digital/digital-to-analog converters (ADCs/DACs).

Existing studies on MiLAC have focused on modelling [3], beamforming design [4], and practical architecture development [5], [6], while channel state information (CSI) acquisition remains an open problem. Accurate CSI is essential for MiLAC-aided beamforming, as it directly determines the configuration of tunable admittance components in MiLACs. Although MiLACs can efficiently perform pre-multiplication of input signal vectors by precoders or combiners in the analog domain, thereby enabling MiLAC-aided beamforming, this capability is insufficient for conventional least squares (LS) and minimum mean square error (MMSE) channel estimation. This is because conventional LS and MMSE require aggregating received signals over multiple training time slots and processing the resulting matrix via operations such as post-multiplication and vectorization [7], which necessitate digital storage and computation beyond the capabilities of MiLACs. Consequently, achieving channel estimation with MiLACs without compromising the advantages of MiLAC-aided beamforming is a non-trivial design challenge.

To address this gap, in this letter, we investigate channel estimation in a point-to-point MIMO system aided by MiLACs. The contributions of this letter are summarized as follows. *First*, we model a MiLAC-aided MIMO system, where the transmitter- and receiver-side MiLACs implement the training precoder and combiner, respectively, to perform channel estimation. *Second*, we propose efficient LS and MMSE channel estimation schemes for the MiLAC-aided system. By designing training precoders and combiners, the columns of the channel estimate are directly obtained at the receive RF chains. This enables LS and MMSE estimation fully in the analog domain, achieving identical performance to their digital counterparts while eliminating digital computation online, reducing the number of transmit RF chains, enabling the use of low-resolution ADCs/DACs, and ensuring unit peak-to-average power ratio (PAPR) per RF chain. *Third*, we present numerical results on normalized mean square error (NMSE) and computational complexity, which verify the performance and efficiency of the proposed schemes.

II. SYSTEM MODEL

We consider a narrowband point-to-point MIMO system aided by a MiLAC at both the transmitter and receiver, as represented in Fig. 1. The N_T -antenna transmitter and N_R -antenna receiver are equipped with L_T and L_R RF chains,

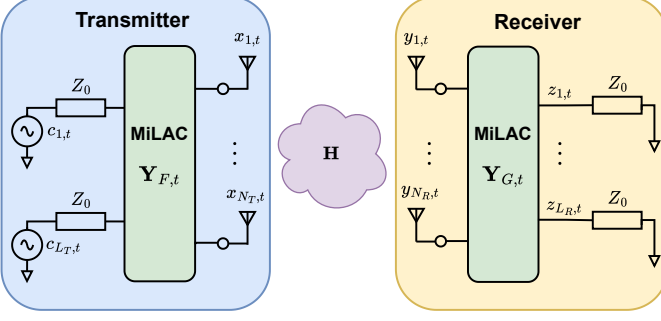


Fig. 1. MiLAC-aided MIMO system model.

respectively, where $L_T \leq N_T$ and $L_R \leq N_R$. Each transmit RF chain is modelled as a voltage generator with series impedance Z_0 (typically 50Ω), while each receive RF chain is modelled as a terminal loaded with Z_0 [8], [9].

As shown in Fig. 1, at the t -th training time slot, $\forall t \in \{1, \dots, \tau\}$, the source signal at transmit RF chains is denoted as $\mathbf{c}_t = [c_{1,t}, \dots, c_{L_T,t}]^T \in \mathbb{C}^{L_T \times 1}$, with $\|\mathbf{c}_t\|^2 = P_T$, where P_T is the transmit power. The source signal \mathbf{c}_t is precoded by the transmitter-side MiLAC, generating the training vector $\mathbf{x}_t = [x_{1,t}, \dots, x_{N_T,t}]^T \in \mathbb{C}^{N_T \times 1}$ at the N_T antennas, written as $\mathbf{x}_t = \mathbf{F}_t \mathbf{c}_t$, where $\mathbf{F}_t \in \mathbb{C}^{N_T \times L_T}$ denotes the training precoder implemented by the transmitter-side MiLAC, satisfying $\sum_{t=1}^{\tau} \|\mathbf{F}_t\|_F^2 = 1$. Referring to [5], [6], the precoder \mathbf{F}_t is a function of the admittance matrix of the transmitter-side MiLAC $\mathbf{Y}_{F,t} \in \mathbb{C}^{(L_T+N_T) \times (L_T+N_T)}$ as

$$\mathbf{F}_t = \left[\left(\frac{\mathbf{Y}_{F,t}}{Y_0} + \mathbf{I}_{L_T+N_T} \right)^{-1} \right]_{L_T+N_T, \mathcal{L}_T}, \quad (1)$$

where $Y_0 = 1/Z_0$ is the reference admittance, and the operator $[\cdot]_{L_T+N_T, \mathcal{L}_T}$ extracts the submatrix composed of the rows and columns with indices $L_T + \mathcal{N}_T = \{L_T + 1, \dots, L_T + N_T\}$ and $\mathcal{L}_T = \{1, \dots, L_T\}$, respectively.

The signal received at the N_R antennas is denoted as $\mathbf{y}_t = [y_{1,t}, \dots, y_{N_R,t}]^T \in \mathbb{C}^{N_R \times 1}$, written as $\mathbf{y}_t = \mathbf{H} \mathbf{x}_t + \mathbf{n}_t$, where $\mathbf{H} \in \mathbb{C}^{N_R \times N_T}$ is the MIMO channel between transmitter and receiver, which is assumed to be quasi-static, i.e., the channel \mathbf{H} remains constant within a coherence block, independent of t [10]. The term $\mathbf{n}_t \in \mathbb{C}^{N_R \times 1}$ denotes the additive white Gaussian noise (AWGN), with $\mathbf{n}_t \sim \mathcal{CN}(\mathbf{0}, \sigma^2 \mathbf{I}_{N_R})$, where σ^2 is the noise power. The signal \mathbf{y}_t is processed by the receiver-side MiLAC, giving the signal at the receive RF chains $\mathbf{z}_t = [z_{1,t}, \dots, z_{L_R,t}]^T \in \mathbb{C}^{L_R \times 1}$ for detection, written as $\mathbf{z}_t = \mathbf{G}_t \mathbf{y}_t$, where $\mathbf{G}_t \in \mathbb{C}^{L_R \times N_R}$ denotes the training combiner implemented by the receiver-side MiLAC. According to [5], [6], the combiner \mathbf{G}_t is a function of the admittance matrix of the receiver-side MiLAC $\mathbf{Y}_{G,t} \in \mathbb{C}^{(N_R+L_R) \times (N_R+L_R)}$ as

$$\mathbf{G}_t = \left[\left(\frac{\mathbf{Y}_{G,t}}{Y_0} + \mathbf{I}_{N_R+L_R} \right)^{-1} \right]_{N_R+\mathcal{L}_R, \mathcal{N}_R}, \quad (2)$$

where the operator $[\cdot]_{N_R+\mathcal{L}_R, \mathcal{N}_R}$ extracts the submatrix composed of the rows and columns with indices $N_R + \mathcal{L}_R = \{N_R + 1, \dots, N_R + L_R\}$ and $\mathcal{N}_R = \{1, \dots, N_R\}$, respectively.

In this letter, we consider MiLACs with unconstrained admittance matrices following [3], [4], which can realize

arbitrary precoder \mathbf{F}_t and combiner \mathbf{G}_t in the analog domain. Hence, any source signal \mathbf{c}_t is equivalent, since the transmitter-side MiLAC can always map it to any training vector \mathbf{x}_t . Without loss of generality, we fix $\mathbf{c}_t = \sqrt{P_T/L_T} \mathbf{1}_{L_T \times 1}$, which distributes power equally across all transmit RF chains and ensures unit PAPR per RF chain, i.e., $\max_t |c_{i,t}|^2 = (1/\tau) \sum_{t=1}^{\tau} |c_{i,t}|^2, \forall i \in \{1, \dots, L_T\}$. Finally, the signal at the receive RF chains at the t -th time slot is

$$\mathbf{z}_t = \sqrt{\frac{P_T}{L_T}} \mathbf{G}_t \mathbf{H} \mathbf{F}_t \mathbf{1}_{L_T \times 1} + \mathbf{G}_t \mathbf{n}_t. \quad (3)$$

In the subsequent sections, we design training precoders \mathbf{F}_t and combiners \mathbf{G}_t over the τ time slots to perform channel estimation. For the ease of exposition, we assume $L_R = N_R$. Under this assumption, at least $\tau \geq N_T$ time slots are required to estimate $N_R N_T$ unknown entries in the channel matrix. Herein, we set $\tau = N_T$ to minimize the training overhead.

III. MILAC-AIDED LS CHANNEL ESTIMATION

In this section, we address LS channel estimation for the MiLAC-aided MIMO system introduced in Section II. Our goal is to perform LS estimation fully in the analog domain, without any digital computation online. This is non-trivial since conventional LS estimation requires forming the received signal matrix and post-multiplying it by the LS estimator, which is beyond the computational capabilities of MiLACs. To address this challenge, we design the training precoder \mathbf{F}_t and combiner \mathbf{G}_t , for $t = 1, \dots, \tau$, such that the t -th column of the LS channel estimate is directly read from the signal \mathbf{z}_t . We then show that MiLACs can exactly implement these precoders and combiners through appropriate admittance design.

A. Training Precoder and Combiner Design

We begin by recalling that the received signal at the t -th time slot is expressed as $\mathbf{y}_t = \mathbf{H} \mathbf{x}_t + \mathbf{n}_t$. By collecting \mathbf{y}_t over the τ time slots, we obtain the received signal matrix $\mathbf{Y} = [\mathbf{y}_1, \dots, \mathbf{y}_\tau] \in \mathbb{C}^{N_R \times \tau}$ as

$$\mathbf{Y} = \mathbf{H} \mathbf{X} + \mathbf{N}, \quad (4)$$

where $\mathbf{X} = [\mathbf{x}_1, \dots, \mathbf{x}_\tau] \in \mathbb{C}^{N_T \times \tau}$ is the training matrix with $\|\mathbf{X}\|_F^2 \leq P_T$, and $\mathbf{N} = [\mathbf{n}_1, \dots, \mathbf{n}_\tau] \in \mathbb{C}^{N_R \times \tau}$ is the noise matrix. The LS estimate of \mathbf{H} is given by

$$\hat{\mathbf{H}}_{\text{LS}} = \mathbf{Y} \mathbf{X}^H (\mathbf{X} \mathbf{X}^H)^{-1}. \quad (5)$$

To minimize the mean square error (MSE) of (5) subject to $\|\mathbf{X}\|_F^2 \leq P_T$, the optimal training matrix must satisfy $\mathbf{X} \mathbf{X}^H = P_T/N_T \mathbf{I}_{N_T}$ [7, Section III]. Without loss of generality, we choose $\mathbf{X} = \sqrt{P_T/N_T} \mathbf{I}_{N_T}$ ¹, so that (5) reduces to

$$\hat{\mathbf{H}}_{\text{LS}} = \sqrt{\frac{N_T}{P_T}} \mathbf{Y}. \quad (6)$$

Under this choice, the training vector at the t -th time slot becomes $\mathbf{x}_t = \sqrt{P_T/N_T} [\mathbf{I}_{N_T}]_{:,t}$. To achieve such \mathbf{x}_t , any

¹Such a design is typically avoided in digital systems because it forces each transmit RF chain to switch between full and zero power, inducing excessively high PAPR. In contrast, this poses no issue in our MiLAC-aided system, since fixing $\mathbf{c}_t = \sqrt{P_T/L_T} \mathbf{1}_{L_T \times 1}$ allows the transmitter-side MiLAC to generate any training vector \mathbf{x}_t while maintaining unit PAPR per RF chain.

training precoder satisfying $\mathbf{F}_t \mathbf{1}_{L_T \times 1} = \sqrt{L_T/N_T} [\mathbf{I}_{N_T}]_{:,t}$ is valid. A simple choice is

$$\mathbf{F}_t = \sqrt{\frac{1}{L_T N_T}} [\mathbf{I}_{N_T}]_{:,t} \mathbf{1}_{1 \times L_T}. \quad (7)$$

Furthermore, to ensure that \mathbf{z}_t equals to the t -th column of the LS channel estimate, i.e., $\mathbf{z}_t = [\hat{\mathbf{H}}_{\text{LS}}]_{:,t}$, we set the training combiner

$$\mathbf{G}_t = \sqrt{\frac{N_T}{P_T}} \mathbf{I}_{N_R}. \quad (8)$$

In summary, the proposed training precoder \mathbf{F}_t and combiner \mathbf{G}_t , for $t = 1, \dots, \tau$, allow the LS channel estimate to be directly obtained at the receive RF chains, without any digital computation online.

B. MiLAC Admittance Matrix Design

We next show that the proposed training precoder \mathbf{F}_t and combiner \mathbf{G}_t , for $t = 1, \dots, \tau$, can be exactly implemented by MiLACs via appropriately designed admittance matrices $\mathbf{Y}_{F,t}$ and $\mathbf{Y}_{G,t}$. Recall that $L_R = N_R$ and $\tau = N_T$ are assumed.

To this end, we first need to find two matrices $\mathbf{Q}_{F,t} \in \mathbb{C}^{(L_T+N_T) \times (L_T+N_T)}$ and $\mathbf{Q}_{G,t} \in \mathbb{C}^{(N_R+L_R) \times (N_R+L_R)}$, with $\mathbf{Q}_{F,t} = (\mathbf{Y}_{F,t}/Y_0 + \mathbf{I}_{L_T+N_T})^{-1}$ and $\mathbf{Q}_{G,t} = (\mathbf{Y}_{G,t}/Y_0 + \mathbf{I}_{N_R+L_R})^{-1}$, whose blocks satisfy $[\mathbf{Q}_{F,t}]_{L_T+N_T, \mathcal{L}_T} = \mathbf{F}_t$ and $[\mathbf{Q}_{G,t}]_{N_R+L_R, N_R} = \mathbf{G}_t$, according to (1) and (2). Since the admittance matrices of MiLACs are assumed unconstrained, the remaining blocks in $\mathbf{Q}_{F,t}$ and $\mathbf{Q}_{G,t}$, apart from the two corresponding to \mathbf{F}_t and \mathbf{G}_t , can take arbitrary complex values as long as $\mathbf{Q}_{F,t}$ and $\mathbf{Q}_{G,t}$ remain invertible. This admits an infinite number of valid solutions, one of which is given by

$$\mathbf{Q}_{F,t} = \begin{bmatrix} \mathbf{I}_{L_T} & \mathbf{0}_{L_T \times N_T} \\ \mathbf{F}_t & \mathbf{I}_{N_T} \end{bmatrix}, \quad \mathbf{Q}_{G,t} = \begin{bmatrix} \mathbf{I}_{N_R} & \mathbf{0}_{N_R \times L_R} \\ \mathbf{G}_t & \mathbf{I}_{L_R} \end{bmatrix}, \quad (9)$$

Using the 2×2 block matrix inversion theorem [11, Theorem 2.1], the corresponding admittance matrices of MiLACs follow

$$\mathbf{Y}_{F,t} = \begin{bmatrix} \mathbf{0}_{L_T \times L_T} & \mathbf{0}_{L_T \times N_T} \\ -Y_0 \mathbf{F}_t & \mathbf{0}_{N_T \times N_T} \end{bmatrix}, \quad (10)$$

$$\mathbf{Y}_{G,t} = \begin{bmatrix} \mathbf{0}_{N_R \times N_R} & \mathbf{0}_{N_R \times L_R} \\ -Y_0 \mathbf{G}_t & \mathbf{0}_{L_R \times L_R} \end{bmatrix}. \quad (11)$$

These results confirm that MiLACs can effectively realize the proposed training precoder \mathbf{F}_t and combiner \mathbf{G}_t , for $t = 1, \dots, \tau$, thereby enabling LS channel estimation to be carried out fully in the analog domain.

C. Comparison with Digital LS Channel Estimation

To facilitate the comparison, we first describe how conventional digital LS channel estimation operates. In digital LS, the identity training matrix $\mathbf{X} = \sqrt{P_T/N_T} \mathbf{I}_{N_T}$ used in MiLAC-aided LS cannot be adopted, because it leads to excessively high PAPR at each transmit RF chain. For this reason, digital LS conventionally adopts a scaled discrete Fourier transform (DFT) training matrix satisfying $\mathbf{X} \mathbf{X}^H = P_T/N_T \mathbf{I}_{N_T}$ [7]. Under this choice, the LS estimator $\mathbf{X}^H (\mathbf{X} \mathbf{X}^H)^{-1}$ reduces to $N_T/P_T \mathbf{X}^H$, which is a full matrix, rather than the identity

weighting $\sqrt{N_T/P_T} \mathbf{I}_{N_R}$ applied in MiLAC-aided LS. Consequently, digital LS must apply the LS estimator to the full received signal matrix \mathbf{Y} to recover the channel.

Compared with digital LS, the proposed MiLAC-aided LS achieves identical estimation performance, since both use training matrices that satisfy the LS optimality condition. Moreover, MiLAC-aided LS greatly reduces computational complexity, requires fewer transmit RF chains, and support low-resolution ADCs/DACs, as summarized below:

1) *Computational Complexity*: Following [3], we define computational complexity as the number of real arithmetic operations performed in the digital domain per coherence block, considering no cost for matrix transpose/Hermitian, and two and six real operations for each complex addition/subtraction and multiplication, respectively. In MiLAC-aided LS, the proposed training precoder \mathbf{F}_t and combiner \mathbf{G}_t , for $t = 1, \dots, \tau$, are predetermined as in (7) and (8), which can be implemented by MiLACs through admittance components precomputed offline [4]. Thus, MiLAC-aided LS requires no real operations online, as all processing is performed in the analog domain. In contrast, given the predetermined DFT training matrix and the corresponding LS estimator, digital LS is dominated by the matrix-matrix multiplication $\mathbf{Y} \mathbf{X}^H$, requiring $8\tau N_R N_T$ real operations².

2) *Number of Transmit RF Chains*: In MiLAC-aided LS, the source signal \mathbf{c}_t is fed into the transmitter-side MiLAC, which generates the training vector \mathbf{x}_t in the analog domain. Since the role of \mathbf{c}_t is only to supply power to the transmitter-side MiLAC, a single transmit RF chain, i.e., $L_T = 1$, is sufficient. In contrast, digital LS generates \mathbf{x}_t in the digital domain, therefore requiring N_T transmit RF chains, one per transmit antenna.

3) *Low-Resolution ADCs/DACs*: In MiLAC-aided LS, both the training vector \mathbf{x}_t and the LS estimate $[\hat{\mathbf{H}}_{\text{LS}}]_{:,t}$ are generated directly in the analog domain. As a result, the transmitter only requires low-resolution DACs to produce the constant source signal \mathbf{c}_t . At the receiver, the ADCs quantize $[\hat{\mathbf{H}}_{\text{LS}}]_{:,t}$, with no need for any subsequent digital computation and therefore no propagation or amplification of quantization distortion, which enables the use of low-resolution ADCs with minimal performance loss [12]. In contrast, digital LS must produce \mathbf{x}_t with high-resolution DACs and quantize the received signal \mathbf{y}_t with high-resolution ADCs to compute the LS estimate digitally, leading to substantially higher hardware cost and power consumption.

IV. MiLAC-AIDED MMSE CHANNEL ESTIMATION

In this section, we introduce MiLAC-aided MMSE channel estimation, which improves performance over MiLAC-aided LS by exploiting channel correlation. This is challenging because conventional MMSE requires collecting received signals over the τ time slots and applying the MMSE estimator to the vectorized received signal matrix, which cannot be supported by MiLACs. To tackle this problem, we begin by characterizing a correlated MIMO channel with the canonical

²A matrix-matrix multiplication \mathbf{AB} with $\mathbf{A} \in \mathbb{C}^{M \times N}$ and $\mathbf{B} \in \mathbb{C}^{N \times L}$ requires approximately $8LMN$ real operations, as detailed in [3, Appendix].

statistical model and assume that the transmit and receive correlation matrices are known. This enables MMSE estimation on the virtual channel, whose correlation matrix is diagonal. By leveraging this diagonal structure, we design the training precoder \mathbf{F}_t and combiner \mathbf{G}_t , for $t = 1, \dots, \tau$, so that MMSE channel estimation is performed fully in the analog domain, without any digital computation online.

A. Channel Model

We consider a correlated MIMO channel described by the canonical statistical model [13]

$$\mathbf{H} = \mathbf{U}_R \mathbf{H}_v \mathbf{U}_T^H, \quad (12)$$

where $\mathbf{U}_T \in \mathbb{C}^{N_T \times N_T}$ and $\mathbf{U}_R \in \mathbb{C}^{N_R \times N_R}$ are unitary matrices containing the eigenvectors of the transmit and receive correlation matrices, $\mathbf{R}_T = \mathbf{U}_T \mathbf{\Lambda}_T \mathbf{U}_T^H$ and $\mathbf{R}_R = \mathbf{U}_R \mathbf{\Lambda}_R \mathbf{U}_R^H$, respectively, while the diagonal matrices $\mathbf{\Lambda}_T \in \mathbb{C}^{N_T \times N_T}$ and $\mathbf{\Lambda}_R \in \mathbb{C}^{N_R \times N_R}$ capture the corresponding eigenvalues. The matrix $\mathbf{H}_v \in \mathbb{C}^{N_R \times N_T}$ denotes the virtual (or eigen-domain) channel, whose entries are zero-mean and uncorrelated with a correlation matrix given by

$$\mathbf{R}_v = \mathbb{E}[\mathbf{h}_v \mathbf{h}_v^H] = \mathbf{\Lambda}_T \otimes \mathbf{\Lambda}_R, \quad (13)$$

where $\mathbf{h}_v = \text{vec}(\mathbf{H}_v) \in \mathbb{C}^{N_R N_T \times 1}$, and we assume \mathbf{R}_v to be full rank, as commonly adopted in the literature [13]–[16].

From (12), \mathbf{H} and \mathbf{H}_v are unitarily equivalent, so MMSE channel estimation can be performed on \mathbf{H}_v rather than \mathbf{H} , without any loss in the MSE [13]. Importantly, the diagonal structure of \mathbf{R}_v greatly simplifies MMSE channel estimation, enabling the training precoder \mathbf{F}_t and combiner \mathbf{G}_t , for $t = 1, \dots, \tau$, to be designed so that the t -th column of the MMSE channel estimate is directly obtained at the signal \mathbf{z}_t , as detailed in Section IV-B.

B. Training Precoder and Combiner Design

Recall that $L_R = N_R$ and $\tau = N_T$ are assumed. Starting from the channel model in (12), (4) can be rewritten as

$$\mathbf{Y}_v = \mathbf{H}_v \mathbf{X}_v + \mathbf{N}_v, \quad (14)$$

where $\mathbf{Y}_v = \mathbf{U}_R^H \mathbf{Y} \in \mathbb{C}^{N_R \times \tau}$, $\mathbf{X}_v = \mathbf{U}_T^H \mathbf{X} \in \mathbb{C}^{N_T \times \tau}$, and $\mathbf{N}_v = \mathbf{U}_R^H \mathbf{N} \in \mathbb{C}^{N_R \times \tau}$. By vectorizing \mathbf{Y}_v , we obtain

$$\mathbf{y}_v = \mathbf{W} \mathbf{h}_v + \mathbf{n}_v, \quad (15)$$

where $\mathbf{y}_v = \text{vec}(\mathbf{Y}_v) \in \mathbb{C}^{\tau N_R \times 1}$ and $\mathbf{n}_v = \text{vec}(\mathbf{N}_v) \in \mathbb{C}^{\tau N_R \times 1}$, with $\mathbf{W} = (\mathbf{X}_v^T \otimes \mathbf{I}_{N_R}) \in \mathbb{C}^{\tau N_R \times N_R N_T}$ following from [17, Theorem 13.26]. The MMSE estimate of \mathbf{h}_v is

$$\hat{\mathbf{h}}_{v, \text{MMSE}} = \mathbf{A} \mathbf{y}_v, \quad (16)$$

where $\mathbf{A} \in \mathbb{C}^{N_R N_T \times \tau N_R}$ is given by

$$\mathbf{A} = \mathbf{R}_v \mathbf{W}^H \left(\mathbf{W} \mathbf{R}_v \mathbf{W}^H + \sigma^2 \mathbf{I}_{\tau N_R} \right)^{-1}. \quad (17)$$

The resulting MSE is expressed as

$$\text{MSE} = \text{tr} \left(\left(\mathbf{R}_v^{-1} + \frac{1}{\sigma^2} \mathbf{W}^H \mathbf{W} \right)^{-1} \right). \quad (18)$$

Given the diagonal structure of \mathbf{R}_v , the optimal \mathbf{X}_v minimizing (18) subject to $\|\mathbf{X}_v\|_F^2 \leq P_T$ must be diagonal [13],

i.e., $\mathbf{X}_v = \text{diag}(\sqrt{p_1}, \dots, \sqrt{p_\tau})$, where p_t denotes the power allocated to the t -th transmit eigen-direction. The optimal power allocation can be obtained by solving

$$\min_{p_t, \forall t} \quad \sum_{t=1}^{\tau} \sum_{j=1}^{N_R} \frac{\sigma^2 [\mathbf{R}_v]_{k,k}}{\sigma^2 + p_t [\mathbf{R}_v]_{k,k}} \quad (19)$$

$$\text{s.t.} \quad \sum_{t=1}^{\tau} p_t \leq P_T, \quad (20)$$

where (19) follows from expanding (18), with $k = (t-1)N_R + j$ ³. Since $\mathbf{X} = \mathbf{U}_T \mathbf{X}_v$, the training vector at t -th time slot is $\mathbf{x}_t = \sqrt{p_t} \mathbf{u}_t$, where $\mathbf{u}_t \in \mathbb{C}^{N_T \times 1}$ denotes the t -th column of the transmit eigenvector matrix \mathbf{U}_T . To generate such \mathbf{x}_t , we set the training precoder

$$\mathbf{F}_t = \sqrt{\frac{p_t}{L_T P_T}} \mathbf{u}_t \mathbf{1}_{1 \times L_T}. \quad (21)$$

Moreover, with both \mathbf{R}_v and \mathbf{X}_v diagonal, the MMSE estimator in (17) becomes diagonal, whose k -th diagonal entry is expressed as

$$[\mathbf{A}]_{k,k} = \frac{\sqrt{p_t} [\mathbf{R}_v]_{k,k}}{\sigma^2 + p_t [\mathbf{R}_v]_{k,k}}. \quad (22)$$

With this entry-wise weighting, to ensure that \mathbf{z}_t equals to the t -th column of the MMSE channel estimate, i.e., $\mathbf{z}_t = [\hat{\mathbf{H}}_{v, \text{MMSE}}]_{:,t}$, we choose the training combiner

$$\mathbf{G}_t = \mathbf{A}_t \mathbf{U}_R^H. \quad (23)$$

where $\mathbf{A}_t = [\mathbf{A}]_{\mathcal{I}_t, \mathcal{I}_t} \in \mathbb{C}^{N_R \times N_R}$ with $\mathcal{I}_t = \{(t-1)N_R + 1, \dots, tN_R\}$.

Overall, the proposed training precoder \mathbf{F}_t and combiner \mathbf{G}_t , for $t = 1, \dots, \tau$, enable the MMSE channel estimate to be directly obtained at the receive RF chains. This process requires no digital computation online, since \mathbf{F}_t and \mathbf{G}_t can be precomputed offline based on the transmit and receive correlation matrices \mathbf{R}_T and \mathbf{R}_R , which vary slowly across coherence blocks [13], [14].

C. Comparison with Digital MMSE Channel Estimation

We can readily verify that MiLACs can realize the proposed training precoder \mathbf{F}_t and combiner \mathbf{G}_t , for $t = 1, \dots, \tau$, since their corresponding admittance matrices follow directly from (10) and (11). Thus, the proposed MiLAC-aided MMSE channel estimation can achieve the same minimum MSE as its digital counterpart, i.e., realizing \mathbf{F}_t and \mathbf{G}_t entirely in the digital domain to obtain the MMSE channel estimate. Moreover, the advantages highlighted in Section III-C, including no real operation online, fewer transmit RF chains, and enabling the use of low-resolution ADCs/DACs, still hold for MiLAC-aided MMSE. In contrast, although \mathbf{F}_t and \mathbf{G}_t are precomputed offline, digital MMSE still requires approximately $8\tau N_R^2$ real operations to compute the matrix-vector multiplication $\mathbf{G}_t \mathbf{y}_t$ over the τ time slots.

³Since (19) involves double summations, a closed-form solution cannot be obtained under conventional water-filling. Instead, it can be efficiently solved via a two-layer water-filling-type method derived from the Lagrange multipliers and Karush–Kuhn–Tucker (KKT) conditions, as detailed in [14].

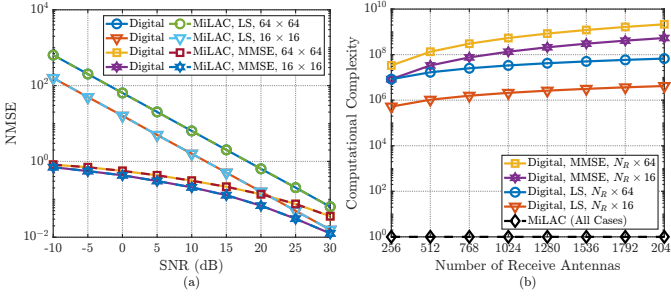


Fig. 2. Comparison of digital and MiLAC-aided channel estimation in an $N_R \times N_T$ MIMO system: (a) NMSE versus SNR; (b) computational complexity versus number of receive antennas.

Notably, MiLAC-aided MMSE also achieves lower PAPR than digital MMSE, as the source signal $\mathbf{c}_t = \sqrt{P_T/L_T} \mathbf{1}_{L_T \times 1}$ always ensures unit PAPR per RF chain. In contrast, digital MMSE employs a training vector \mathbf{x}_t at the N_T transmit RF chains with significant power fluctuations, since strong power is allocated to dominant transmit eigen-directions while weak ones receive almost none. This yields high PAPR, degrading power amplifier efficiency and causing nonlinear distortion.

V. NUMERICAL RESULTS

In this section, we present simulation results to evaluate the performance of the proposed MiLAC-aided LS and MMSE channel estimation and to quantify their benefits in terms of computational complexity, compared with their digital counterparts. To this end, we assume that the transmit and receive correlation matrices, \mathbf{R}_T and \mathbf{R}_R , follow the widely adopted exponential correlation model [7], [13], [14], expressed as $[\mathbf{R}_T]_{i,j} = \epsilon_T^{|i-j|}$, $[\mathbf{R}_R]_{i,j} = \epsilon_R^{|i-j|}$, where $0 \leq \epsilon_T < 1$, $0 \leq \epsilon_R < 1$ denote the transmit and receive correlation coefficient. Herein, we set $\epsilon_T = \epsilon_R = 0.8$ to characterize strongly correlated MIMO channels.

Fig. 2a presents the NMSE = $\mathbb{E}\{||\mathbf{H} - \hat{\mathbf{H}}||_F^2\}/\mathbb{E}\{||\mathbf{H}||_F^2\} = \mathbb{E}\{||\mathbf{H}_v - \hat{\mathbf{H}}_v||_F^2\}/\mathbb{E}\{||\mathbf{H}_v||_F^2\}$ versus the SNR = P_T/σ^2 achieved by digital and MiLAC-aided LS and MMSE channel estimation, where $N_T = N_R \in \{16, 64\}$. As expected, LS estimation suffers from higher NMSE, especially at low SNR, while MMSE estimation achieves improved performance by exploiting channel statistics. A slightly higher NMSE is observed for larger antenna numbers, as the total transmit power P_T is fixed. Notably, MiLAC-aided LS and MMSE consistently achieve the same estimation performance as their digital counterparts across varying antenna numbers, validating our theoretical insights in Sections III and IV.

Fig. 2b evaluates the computational complexity of digital and MiLAC-aided LS and MMSE channel estimation as a function of N_R , varying from 256 to 2048, with $N_T \in \{16, 64\}$. We have the following observations. *First*, digital MMSE requires more computation than digital LS, since its complexity $8\tau N_R^2$ grows quadratically with N_R , while digital LS scales as $8\tau N_R N_T$, linearly with N_R but quadratically with N_T , since $\tau = N_T$. This explains why increasing N_T results in a sharper complexity rise for digital LS. *Second*, MiLAC-aided LS and MMSE require no digital computation

online, saving up to 2.15×10^9 real operations when MMSE estimation is applied in a 2048×64 MIMO system, which implies much lower processing latency and power consumption.

VI. CONCLUSION

In this letter, we propose efficient LS and MMSE channel estimation schemes for MiLAC-aided MIMO systems. These schemes enable conventional LS and MMSE estimation, which rely on intensive digital computation, to be performed entirely in the analog domain, achieving the same performance as their digital counterparts while greatly reducing computational complexity, transmit RF chains, ADCs/DACs resolution requirements, and PAPR. These results highlight that MiLAC can provide a practical pathway toward real-time and energy-efficient channel estimation in future gigantic MIMO systems.

REFERENCES

- [1] E. Björnson, F. Kara, N. Kolomvakis, A. Kosasih, P. Ramezani, and M. B. Salman, "Enabling 6G performance in the upper mid-band by transitioning from massive to gigantic MIMO," *IEEE Open J. Commun. Soc.*, vol. 6, pp. 5450–5463, 2025.
- [2] E. G. Larsson, O. Edfors, F. Tufvesson, and T. L. Marzetta, "Massive MIMO for next generation wireless systems," *IEEE Commun. Mag.*, vol. 52, no. 2, pp. 186–195, 2014.
- [3] M. Nerini and B. Clerckx, "Analog computing for signal processing and communications – part I: Computing with microwave networks," 2025. [Online]. Available: <https://arxiv.org/abs/2504.06790>
- [4] ———, "Analog computing for signal processing and communications – part II: Toward gigantic mimo beamforming," 2025. [Online]. Available: <https://arxiv.org/abs/2504.07477>
- [5] ———, "Capacity of MIMO systems aided by microwave linear analog computers (MiLACs)," 2025. [Online]. Available: <https://arxiv.org/abs/2506.05983>
- [6] ———, "MIMO systems aided by microwave linear analog computers: Capacity-achieving architectures with reduced circuit complexity," 2025. [Online]. Available: <https://arxiv.org/abs/2506.15052>
- [7] M. Biguesh and A. Gershman, "Training-based MIMO channel estimation: a study of estimator tradeoffs and optimal training signals," *IEEE Trans. Signal Process.*, vol. 54, no. 3, pp. 884–893, 2006.
- [8] M. T. Ivrlač and J. A. Nossek, "Toward a circuit theory of communication," *IEEE Trans. Circuits Syst. I, Reg. Papers*, vol. 57, no. 7, pp. 1663–1683, 2010.
- [9] M. Nerini, S. Shen, H. Li, M. Di Renzo, and B. Clerckx, "A universal framework for multiport network analysis of reconfigurable intelligent surfaces," *IEEE Trans. Wireless Commun.*, vol. 23, no. 10, pp. 14 575–14 590, 2024.
- [10] D. Tse and P. Viswanath, *Fundamentals of wireless communication*. Cambridge: Cambridge University Press, 2005.
- [11] T.-T. Lu and S.-H. Shiu, "Inverses of 2×2 block matrices," *Computers & Mathematics with Applications*, vol. 43, no. 1, pp. 119–129, 2002. [Online]. Available: <https://www.sciencedirect.com/science/article/pii/S0898122101001028>
- [12] N. Shlezinger, Y. C. Eldar, and M. R. D. Rodrigues, "Hardware-limited task-based quantization," *IEEE Transactions on Signal Processing*, vol. 67, no. 20, pp. 5223–5238, 2019.
- [13] J. Kotecha and A. Sayeed, "Transmit signal design for optimal estimation of correlated MIMO channels," *IEEE Trans. Signal Process.*, vol. 52, no. 2, pp. 546–557, 2004.
- [14] J. Mirzaei, S. ShahbazPanahi, F. Sohrabi, and R. Adve, "Hybrid analog and digital beamforming design for channel estimation in correlated massive MIMO systems," *IEEE Trans. Signal Process.*, vol. 69, pp. 5784–5800, 2021.
- [15] W. Weichselberger, M. Herdin, H. Ozcelik, and E. Bonek, "A stochastic MIMO channel model with joint correlation of both link ends," *IEEE Trans. Wireless Commun.*, vol. 5, no. 1, pp. 90–100, 2006.
- [16] B. Clerckx and C. Oestges, *MIMO wireless networks channels, techniques and standards for multi-antenna, multi-user and multi-cell systems*, 2nd ed. Burlington: Elsevier Science, 2013.
- [17] A. J. Laub, *Matrix Analysis for Scientists and Engineers*. Philadelphia, PA: Society for Industrial and Applied Mathematics, 2004. [Online]. Available: <https://epubs.siam.org/doi/abs/10.1137/1.9780898717907>